Impact of a Circular Cylinder on a Water Surface
(Preliminary Study on Computational Analysis)

Toshio NISHIMURA*[1], Yoshiaki UEDA*[1], Shoki YONAMINE*[1], Ryoji TSUJINO*[1] and Manabu IGUCHI*[2]

*1 Department of Mechanical Engineering, Setsunan University
17-8 Ikedanaka-machi, Neyagawa, Osaka 572-8508, JAPAN
13M305nt@edu.setsunan.ac.jp, y-ueda@eng.hokudai.ac.jp,
104138ys@edu.setsunan.ac.jp, tsujino@mec.setsunan.ac.jp

*2 Department of Mechanical Engineering, Osaka Electro-Communication University
18-8 Hatsucho, Neyagawa, Osaka 572-8530, JAPAN
gaku@eng.hokudai.ac.jp

Abstract
This paper aims to investigate the impact of a circular cylinder on a water surface. The equation of motion of the sinking cylinder is numerically solved with the first-order Euler method. The hydrodynamic force exerted on the wetted surface of the cylinder is then estimated by (1) a usual steady drag force (C_D = 1.15) for a circular cylinder and (2) the FLUENT computation for a cylinder partially immersed in water. The results of these strategies (1) and (2) are compared and discussed for several kinds of the density ratios including low- and high-density cylinders. In particular, the hydrodynamic force needs to be estimated exactly during the impact where the high-density cylinder is partially immersed.
Keywords: water entry, multi-phase flow, CFD, two-dimensional, two-way coupling

1 Introduction
In a steelmaking process, the micro particles such as calcium oxide (CaO, desulphurization chemical) should be effectively injected into a molten iron bath (solid-liquid impact) and dispersed in the whole bath to enhance the efficiency of desulphurization or dephosphorization (see **Fig. 1**). However, the injected particles attract gas bubbles due to the poor wettability with molten iron so that the dispersion in the bath could be inhibited [1]. To achieve the effective dispersion of the injected particles, we need to investigate the dynamic behaviors of the particle motion and its air cavity formed by the liquid entry of particles.

Pioneering work of solid-liquid impact can be found in Worthington & Cole [2] who used single-spark photography to examine the air cavity formed by the entry of a sphere into water. Recently, with the progress of a high-speed camera, several kinds of articles visually investigate the air cavity formed by a superhydrophobic sphere entering into water (see e.g., [3,4,5]).

Among possible numerical approaches, one can cite the boundary element method (BEM) and the level-set method. This latter procedure was successfully implemented in Zhang et al. [6] to compute the impact of a circular cylinder on a water surface. Also, the Volume-of-Fluid (VOF) method was successfully done in Lin [7] and Mnasri et al. [8] (through the dynamic mesh routine of the FLUENT^{TM} commercial code) to compute the water entry and exit of a circular cylinder. In these computations, a two-way coupling is required for successful simulation. Even with the recent progress of computer hardware, there are very few studies which achieve an accurate two-way coupling computation in such a problem of a cluster of particles.

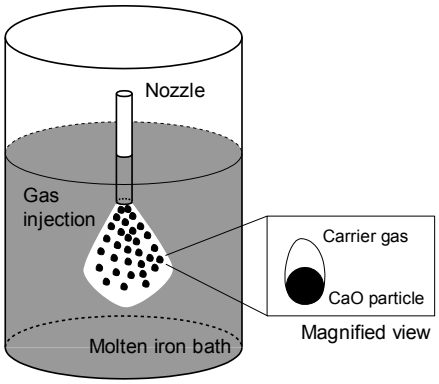

Fig. 1 Sketch of injection of micro particles, with carrier gas, into a molten iron bath in a steelmaking process

The present study aims to computationally investigate the impact of a circular cylinder on a water surface (as 2D problem), as a preliminary study for liquid entry- and exit-problem of a cluster of particles from gas to liquid surface. In this study, a cluster of CaO particles are modeled by circular cylinders having various densities, carrier gas is by air, and molten iron is by water because of the same kinematic viscosity.

2 Problem Statement and Computational Strategy
2.1 Previous study on water entry of a sphere
Figure 2 shows the instantaneous photographs of hydrophilic and hydrophobic spheres entering into water. As shown in Fig.2, the entry of the hydrophobic sphere into water forms the air cavity whereas the non-coating (polished hydrophilic surface) sphere seems not to form

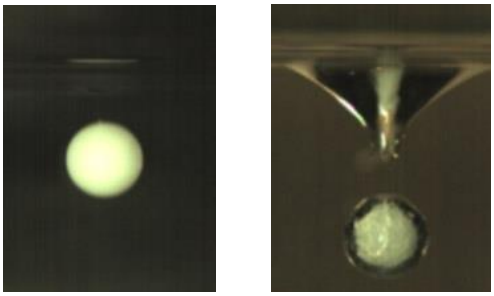

(a) Hydrophilic (b) Hydrophobic

Fig. 2 Influence of surface wettability of a sphere entering into water. Left: Polished acrylic sphere, Right: Acrylic sphere with hydrophobic coating

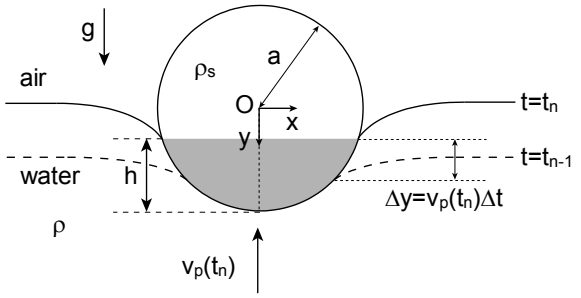

Fig. 3 Coordinate system and problem setting

it.

The underwater cavity formation behind a sphere entering into water surface affects the trajectory of the sinking sphere. Duez et al. [5] examined a threshold velocity U^* of the sphere for air entrainment in terms of equilibrium contact angle θ_c of the impacting sphere where the air cavity is created above U^* (see Fig. 2 of their paper [5]).

Furthermore, the studies of Aristoff *et al*. [9] and Ueda *et al*. [10] address the deceleration of a sphere entering into water, and, therefore, it can be found that the two-way coupling is required for accurate simulation of the present water-entry problem.

2.2 Problem setting

At $t = 0$, a falling circular cylinder impacts on a water surface with the initial velocity v_{p0}. Then, the cylinder penetrates the water surface due to the inertia force of itself and makes the splash on the water surface. As mentioned in the last subsection, a low-density cylinder rapidly decelerates after the impact due to the buoyancy and hydrodynamic forces, whereas a high-density cylinder approximately keeps the initial velocity v_{p0} due to the large inertia force (see e.g., [3]).

The equation of motion for the cylinder entering into water can be described as follows:

$$(m + m_a)\ddot{Z}_c = mg - F_b - F_c - F_h \tag{1}$$

in which Z_c is the center of the cylinder from the static free surface level, m the mass of the sphere and m_a the added mass. In addition, F_b is the upward buoyancy force due to the hydrostatic pressure acting over the wetted surface of the sphere, F_c is the upward force due to the surface tension, and F_h is the upward hydrodynamic residence force. In general, for a high Froude number impact (i.e., a high-speed impact), F_c would be sufficiently smaller than other forces and thus it could be negligible. The buoyancy force F_b can be readily calculated through the wetted area of a cylinder (i.e., shaded area of **Fig. 3** contributes F_b). Therefore, without the influence of splash on the liquid surface, the hydrodynamic force F_h is found to be the key term to solve the equation of motion (1) and F_h can be assumed to be exerted by the wetted surface of the cylinder.

All laws of classical Newtonian physics are well known to be Galilean invariant and, therefore, the present situation can be switched to the relative coordinate system fixed with the center of the falling circular cylinder (see Fig. 3), i.e., the circular cylinder is fixed at the origin, and the free surface level moves upward with the velocity $v_p(t) = \mathrm{d}Z_c/\mathrm{d}t$.

2.3 Computational procedure

The FLUENT numerical code ver.13.0, a commercially available Computational Fluid Dynamics (CFD) software package, was employed for all numerical predictions on 3.60GHz Intel Core i7 Processor with 16GB RAM. ICEMCFD™ ver.13.0 was employed for the establishment of the two-dimensional computational grid. The computational grids were made up of 1,152,302 cells for entire flow domain.

FLUENT uses a control-volume-based technique to solve the governing continuity and momentum equations. A segregated implicit solver and first-order upwind interpolation scheme were employed for each computational iteration. A time-step size of Δt = 0.001(s) was adopted to achieve a convergence in every time step. The convergence of the computational solution was determined based on residuals for the continuity and x-, y-, z-velocities. The residual of all quantities was set to 10^{-3}. The solution was considered to be converged when all of the residuals were less than or equal to these default settings (see FLUENT User's Guide [11] for more details).

FLUENT offers the dynamic mesh to simulate a moving body problem such as the present water-entry situation. The application of the dynamic mesh will be briefly mentioned below.

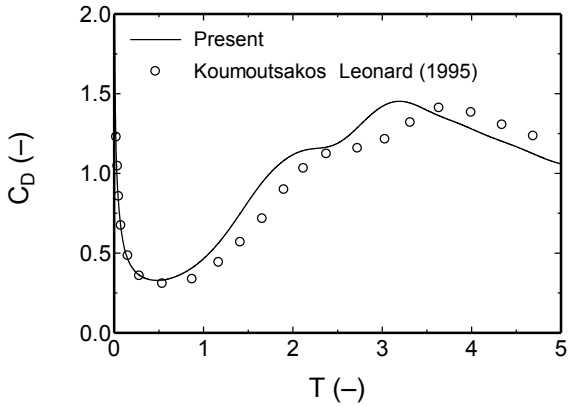

Fig. 4 Comparison of transient drag coefficient C_D of a circular cylinder fully immersed in liquid at Re = 3000 betwe & Leonard [12]

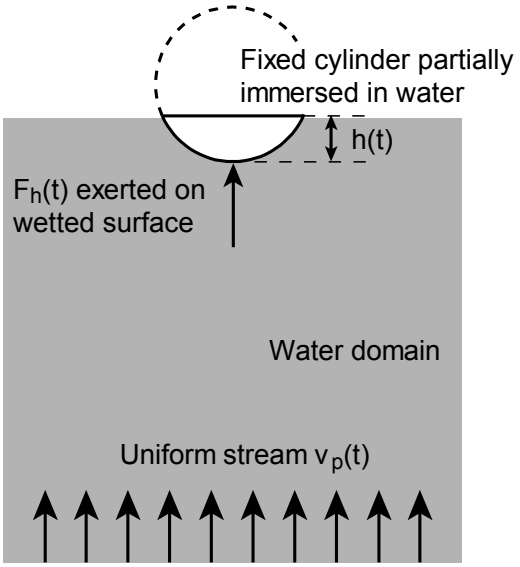

Fig. 5 Computation of hydrodynamic force F_h at time t.

2.4 Computational benchmark of an impulsively started circular cylinder fully immersed in liquid

The transient problem of a circular cylinder fully immersed in liquid makes it possible to verify the present grid resolution against the earlier results [12]. Taking into account the actual situation mentioned in the introduction, we here set the Reynolds number at 3000. The grid adopted is 30D x 50D in the entire flow domain (15D in upward, and 25D in downward) and 600 discretized grids around the cylinder surface. The time increment is set at $\Delta t = 0.001$ to satisfy the Courant condition.

Figure 4 shows the comparison of the drag coefficient C_D at the early stage of motion between the present computation and Koumoutsakos & Leonard [12]. In Fig.4, the present computation seems to be almost agreement with the earlier result [12].

3 Results and Discussion

As mentioned in Subsection 2.2, the estimation of the hydrodynamic force F_h mainly exerted on the wetted surface of the cylinder is the key to solve the equation of motion (1). To do so, we consider the situation at time t, where the circular cylinder is partially immersed in water (see Fig. 3). In practice, we carry out the following routine 1 to 3:

(1) At time $t = t_n$, F_h is calculated for the situation of Fig.3.
(2) The equation of motion (1) is then numerically solved using the first-order Euler method with the calculated buoyancy force, and therefore the depth of the cylinder in water at $t_{n+1} = t_n + \Delta t$ can be advanced.
(3) Repeatedly going on the routine 1 and the time progresses.

To calculate F_h on the wetted surface of the cylinder, we deal with a couple of strategies mentioned in the following Subsections 3.1 and 3.2.

3.1 Calculation with the usual steady drag force

To avoid the difficulty of the calculation of F_h on the wetted surface, the first strategy employs the steady drag coefficient which was given in [13] for a fully immersed circular cylinder (C_D = 1.15). Then, F_h is calculated by $F_h = (1/2)\rho v_p(t)^2 a C_D$ as a function of the variable $v_p(t)$ during the penetration of the water surface (see Fig.3). Here, ρ is the density of water, and a the radius of the cylinder. In this procedure, after the high-density cylinder fully enters into water, the sinking velocity of the cylinder ends up settling to the terminal velocity $U_T = [2\pi ag(\rho_s/\rho\text{-}1)]^{1/2}$ where the gravitational force mg balances with F_b and F_h .

To test this strategy, we select the four sets of the conditions for this water-entry problem. The initial impact velocity v_{p0} on the water surface is fixed at 1.0 (m/s), the cylinder has the diameter of $d = 2a = 10$ (mm), and the densities of the cylinder ρ_s are varied as (i) 200 (kg/m^3), (ii) 500 (kg/m^3), (iii) 1500 (kg/m^3) and (iv) 2700 (kg/m^3) against the density of water ρ = 1000 (kg/m^3).

The results are given in the following subsections compared with the second strategy.

3.2 Calculation with computational results of F_h

As mentioned before, the circular cylinder partially immersed in water is mainly exerted on not the dry surface but the wetted surface (remind the situation of Fig. 3) because the density ratio between water and air is approximately 1000. Therefore, the second strategy uses the value of F_h obtained by the unsteady FLUENT computation for the situation of Fig. 5 (i.e., the computational domain consists of the shaded area in Fig. 5). After the routine 2, the computational grid needs to be reconstructed for advancing the depth of the cylinder in water.

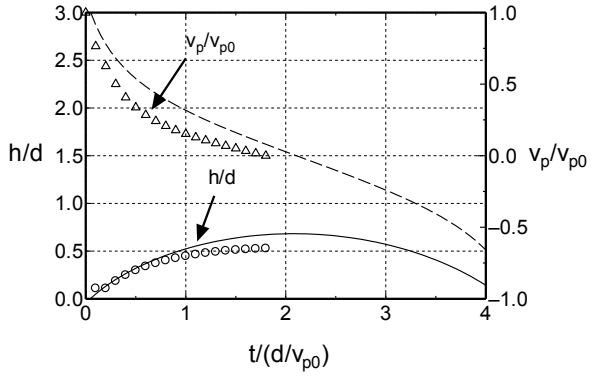

Fig. 6 Comparison of h/d and v_p/v_{p0} at ρ_s/ρ = 0.2 between the strategies 1 (line) and 2 (mark).

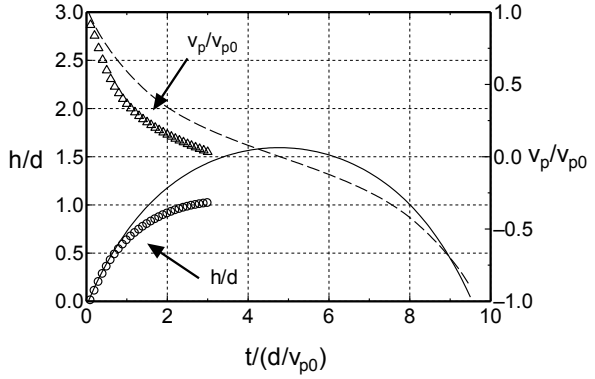

Fig. 7 Comparison of h/d and v_p/v_{p0} at ρ_s/ρ = 0.5 between the strategies 1 (line) and 2 (mark).

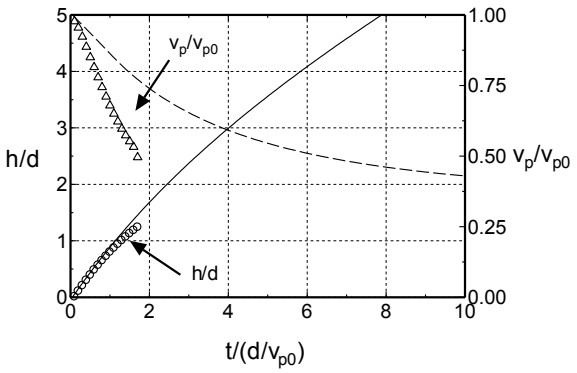

Fig. 8 Comparison of h/d and v_p/v_{p0} at ρ_s/ρ = 1.5 between the strategies 1 (line) and 2 (mark).

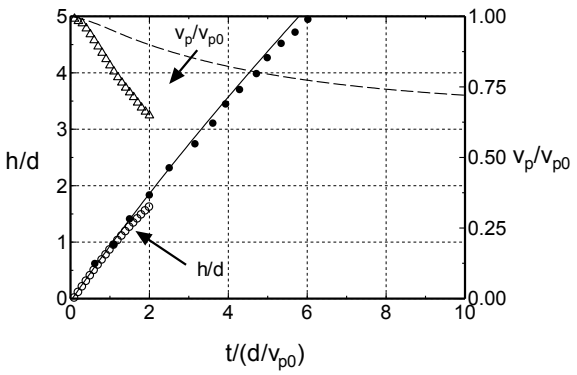

Fig. 9 Comparison of h/d and v_p/v_{p0} at ρ_s/ρ = 2.7 between the strategies 1 (line) and 2 (open mark), together with the previous experimental result [14] (solid circle).

For low-density cylinders: Figures 6 and **7** show the time dependent of the dimensionless depth h/d and the sinking velocity v_p/v_{p0} for two values of the density ratios, ρ_s/ρ = 0.2 and 0.5. The computation of the strategy 2 stops at the sinking velocity being less than zero, whereas the routine of the strategy 1 continues to be more. In these figures, it seems that the results of the strategy 1 agree well with that of the strategy 2 for the low density cylinder (ρ_s/ρ = 0.2).

After the impact, the low-density cylinder decelerates due to the hydrodynamic (F_h) and buoyancy (F_b) forces, and the sinking velocity of the cylinder v_p settles to zero. Before the settlement of the cylinder, the circular cylinder penetrates to some extent the water surface due to the initial inertia force, even if the cylinder density is less than the water density. As seen in Fig.6, the maximum depth of the cylinder h is at most less than d for ρ_s/ρ = 0.2, whereas the cylinder approximately reaches h = 1.1d for ρ_s/ρ = 0.5 in **Fig. 7**.

For high-density cylinders: Figures 8 and **9** show the time dependent of the dimensionless depth h/d and the sinking velocity v_p/v_{p0} for two values of ρ_s/ρ = 1.5 and 2.7. The computation of the strategy 2 stops to some extent after the cylinder fully immersed in water due to lots of computational iteration. As observed in Fig. 9, the results of h/d are in good agreement with the previous experimental results [14] in ρ_s/ρ = 2.56 (aluminum circular cylinder). Furthermore, as seen in **Figs. 8** and **9**, the values of h/d are almost identical between the strategies 1 and 2 and, however, the calculated results for v_p/v_{p0} of the strategy 1 are sufficiently larger than that of the strategy 2. In contrast to the impact of a low-density cylinder, the large hydrodynamic force F_h acts on the high-density cylinders due to the large inertia force (see **Fig. 10**) and, therefore, the hydrodynamic force F_h needs to be estimated exactly during the impact where the cylinder is partially immersed. It could be concluded that the rough estimation of F_h in the strategy 1 would yield the remarkable error in the calculation of v_p/v_{p0} between the strategies 1 and 2.

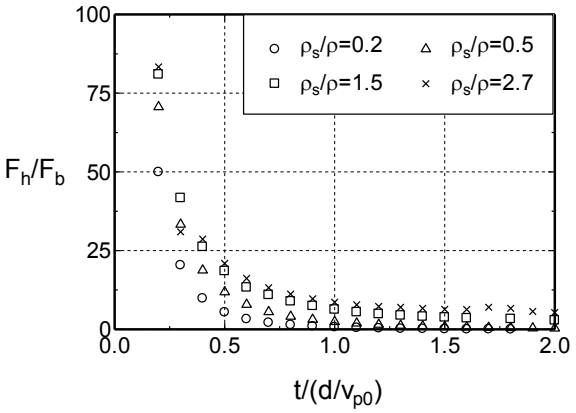

Fig. 10 Computed F_h/F_b in strategy 2 for ρ_s/ρ = 0.2, 0.5, 1.5 and 2.7

3.3 Direct computation with dynamic mesh technique

To accomplish the direct simulation such a water-entry problem, FLUENT offers *dynamic mesh* technique which adjusts the mesh around a moving body in every time step (see Fig. 11). We intend to present the two-way coupling computation using the dynamic mesh procedure in the conference site.

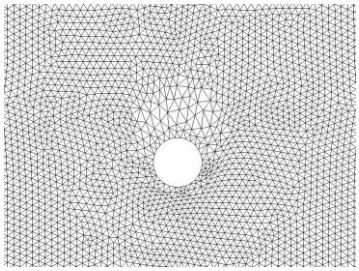

Fig. 11 Example of the dynamic mesh around a sinking circular cylinder

4 Concluding Remarks

This paper has studied the impact of a circular cylinder on a water surface, solving the equation of motion of the cylinder. In general, a computational procedure with a two-way coupling is required for a numerical simulation of such an impact problem. In this study, to avoid the difficulty of the two-way coupling, the hydrodynamic force exerted on the cylinder surface was estimated by (strategy 1) a usual steady drag force (C_D = 1.15) and (strategy 2) the FLUENT computation for a cylinder partially immersed in water.

As a result, the FLUENT computation of the strategy 2 gave appropriate results for a high-density cylinder against the previous experimental result [14]. Although the strategy 1 successfully gave good results for a low-density cylinder, it is not in agreement with the strategy 2 for the results of the sinking velocity of a high-density cylinder having the large inertia force. Therefore, the hydrodynamic force needs to be estimated exactly during the impact where the high-density cylinder is partially immersed.

References

[1] Iguchi, M. and Ilegbusi, O.J., "Modeling multiphase materials processes", Springer, (2011).

[2] Worthington, A.M. and Cole, R.S., "Impact with a liquid surface, studied by the aid of instantaneous photography", Philos. R. Soc. Lond., (Paper I) Vol. 189, (1897), pp. 137-148, (Paper II) Vol. 194, (1900), pp. 175-199.

[3] Aristoff, J.M. and Bush, J.W.M., "Water entry of small hydrophobic spheres", J. Fluid Mech., Vol. 619, (2009), pp. 45-78.

[4] Duclaux, V., Caille, F., Duez, C., Ybert, C., Bocquet, L. and Clanet, C., "Dynamics of transient cavities", J. Fluid Mech., Vol. 591, (2007), pp. 1-19.

[5] Duez, C., Ybert, C., Clanet, C. and Bocquet, L., "Making splash with ater repellency", Nat. Phys., Vol. 3, (2007), pp. 180-183.

[6] Zhang, Y., Zou, Q., Greaves, D., Reeve, D., Hunt-Raby, A., Graham, D., James, P. and Lv, X., "A level set immersed boundary method for water entry and exit", Commun. Comput. Phys., Vol. 8, No.2, (2010), pp. 265-288.

[7] Lin, P.Z., "A fixed grid model for simulation of a moving body in free surface flows", Comput. Fluids., Vol. 36, (2007), pp. 549-561.

[8] Mnasri, C., Hafsia, Z., Omri, M. and Maalel, K., "Free surface behavior induced by horizontal cylinders exit and entry", Eng. Appl. Comput. Mech., Vol. 4, (2010), pp. 260-275.

[9] Aristoff, J.M., Truscott, T.T., Techet, A.H. and Bush, J.W.M., "The water entry of decelerating spheres", Phys. Fluids, Vol. 22, (2010), 032102.

[10] Ueda, Y., Tanaka, M., Uemura, T. and Iguchi, M., "Water entry of a superhydrophobic low-density sphere", J. Vis., Vol. 13, (2010), pp.289-292.

[11] FLUENT 6.2 User's Guide, FLUENT Inc., Lebanon, NH, (2005).

[12] Koumoutsakos, P. and Leonard, A., "High-resolution simulations of the flow around an impulsively started cylinder using vortex methods", J. Fluid Mech., Vol. 296, (1995), pp. l-38.

[13] The Japan Society of Fluid Mechanics, "Handbook of fluid mechanics", 2nd edn, Maruzen, (1998), Chap. 10, pp.442-443.

[14] Ueda, Y. and Iguchi, M., "Rupture of cavity film due to water entry of horizontal superhydrophobic circular cylinders", High Temp. Mater. Proc., (2012), DOI 10.1515/htmp-2012-0060.

Received on November 30, 2013

Accepted on January 27, 2014